Journal of Applied Polymer Science

Enhancement of Mechanical and Tribological Properties in Ring-Opening Metathesis Polymerization Functionalized Molybdenum Disulfide/Polydicyclopentadiene Nanocomposites

Shuge Peng, Yongping Niu, Xinjie Fan

Key Laboratory of Polymer and Nanomaterials, Henan University of Science and Technology, Luoyang 471003, People's Republic of China

Correspondence to: S. Peng (E-mail: sgpeng@mail.haust.edu.cn)

ABSTRACT: This study focuses on the possibility of improving performance properties of polydicyclopentadiene (PDCPD) nanocomposites for engineering applications using nanoparticles. In this article, molybdenum disulfide/polydicyclopentadiene (MoS_2/PDCPD) nanocomposites have been prepared by *in situ* ring-opening metathesis polymerization using reaction injecting molding (RIM) process. To enhance the interfacial adhesion between the fillers and PDCPD matrix, the surface modified MoS_2 nanoparticles hybridized with dialkyldithiophosphate (PyDDP) were successfully prepared by *in situ* surface grafting method. The effect of low MoS_2 loadings (<3 wt %) on the mechanical and tribological behaviors of PDCPD was evaluated. The results indicated that the friction coefficient of the MoS_2/PDCPD nanocomposites was obviously decreased and the wear resistance of nanocomposites was greatly improved by the addition of PyDDP-hybridized MoS_2 nanoparticles; meanwhile, the mechanical properties were also enhanced. The MoS_2/PDCPD nanocomposites filled with 1 wt % PyDDP-hybridized MoS_2 exhibited the best mechanical and anti-wear properties. The friction coefficient was shown to decrease by more than 40% compared to pure PDCPD by incorporating just 1 wt % hybridized MoS_2 nanoparticles, and modest increase in modulus and strength was also observed. The reinforcing and wear-resistant mechanisms of MoS_2/PDCPD nanocomposites were investigated and discussed by scanning electron microscopy. The well interfacial compatibility between the particle/matrix interfaces played an important role for the improved mechanical and tribological properties of MoS_2/PDCPD nanocomposites in very low MoS_2 loadings. © 2012 Wiley Periodicals, Inc. J. Appl. Polym. Sci. 129: 1045–1052, 2013

KEYWORDS: friction; wear and lubrication; mechanical properties; nanoparticles; nanowires and nanocrystals; ring-opening polymerization

Received 9 July 2012; accepted 25 October 2012; published online 22 November 2012
DOI: 10.1002/app.38776

INTRODUCTION

Nowadays, high-performance polymer composite materials are used increasingly for engineering applications under drastic conditions, which demand the materials must provide unique mechanical and tribological properties to ensure safety and economic efficiency. When the polymer matrix must withstand high mechanical and tribological loads, it is usually reinforced with various fillers, such as clay,[1] carbon nanotubes,[2] mesoporous silica,[3] grapheme,[4] fibers,[5] or inorganic nanoparticles.[6,7] In recent years, there is a great interest in polymer/inorganic particles nanocomposites, since they exhibit unique properties, that is, improved mechanical and thermal properties,[8] tribological properties,[9–12] and fire retardance[13] compared to pristine polymer. These enhanced properties can be achieved by adequately dispersing inorganic nanoparticles or layered clay particles within polymer matrix. Therefore, improving the dispersion of inorganic nanoparticles within polymer matrix has become one of the important and difficult points to reinforce and toughen polymers.[14–17]

Polydicyclopentadiene (PDCPD) is a crosslinked polymer formed by ring-opening metathesis polymerization (ROMP) of its bicyclic olefin monomer.[18] PDCPD has become a novel engineering plastic due to its high modulus, excellent impact strength, and chemical resistance since 1990s. These features, along with its quality surface, low-cost, and processability, are leading to widespread use of PDCPD in high-performance composite structures as a matrix material.[19] The related works in constructing high-performance PDCPD composites mainly focus on the enhancement of the mechanical[20,21] and flame-retardant properties.[22,23] Actually, the friction and wear behaviors of pure PDCPD are poor due to the low surface hardness and poor supporting capacity. However, the research on the tribological

behavior of the PDCPD composites is relatively few.[24] It is well known that layered molybdenum disulfide (MoS_2), especially nanosized MoS_2, has considerable applications in many fields such as solid lubrication, lubrication additives in oils, and self-lubricating polymer materials.[25,26] The MoS_2/PDCPD nanocomposites are expected to combine the rigidity, dimensional stability, and wear resistance of MoS_2, with the processability and the favorable properties, such as the mechanical property of pure PDCPD. If inorganic fillers could be well-dispersed in PDCPD matrix, the PDCPD-based composite materials with outstanding comprehensive properties would be expected; meanwhile, the additive amount of the inorganic fillers could be greatly reduced. Based on the research ideas, the well oil-soluble MoS_2 nanoparticles in dicyclopentadiene (DCPD) were designed and prepared; and the MoS_2 nanoparticles with wear resistance were used as the fillers of the PDCPD matrix. It is expected that this work can be useful in promoting the applications of MoS_2/PDCPD nanocomposites under oil-free lubrication conditions.

EXPERIMENTAL

Materials

Diethyl aluminum chloride (Et_2AlCl) and DCPD were purchased from Sinopharm Chemical Reagent Co. Ltd. and used without further purification. Tungsten complex and dialkyldithiophosphate (PyDDP) were synthesized according to the literatures. All the other reagents and solvents were purchased from commercial suppliers and used as received. Deionized water was distilled by water purification system.

PyDDP-Hybridized MoS_2 Fillers

The PyDDP-hybridized MoS_2 fillers were prepared by *in situ* surface grafting method similar to the procedure described by Zhang et al.[27] Typically, 2.4 g $Na_2MoO_4 \cdot 2H_2O$ was dissolved into 100 mL deionized water at 80°C; then, 0.35 g $NH_2OH \cdot$ HCl was added gently and stirred for 1 h, followed by the addition of 30 mL of PyDDP (0.7 g) acetone solution and 10 mL of $Na_2S \cdot 9H_2O$ (7.2 g) aqueous solution. The mixed solution was magnetically stirred for 2 h at 65°C. Finally, the pH value of solution was adjusted to 4 by sulfuric acid and stirred for another 2 h. The PyDDP-hybridized MoS_2 nanoparticles could be collected by filtration and washed thoroughly with deionized water to remove the excess salt. The powder was then dried under vacuum for 10 h at 80°C and subsequently ground into a fine powder.

Preparation of MoS_2/PDCPD Nanocomposites

The MoS_2/PDCPD nanocomposites were prepared by reaction injecting molding (RIM). Figure 1 shows the simulating RIM device in our lab. The general procedure was as follows: A certain amount of PyDDP-hybridized MoS_2 nanoparticles was dispersed uniformly in 100 mL DCPD; then, the dispersion was divided equally and was poured into the two steel tanks under nitrogen atmosphere, respectively. Next, the main catalyst (tungsten complex) and cocatalyst (Et_2AlCl) were injected into the two steel tanks with the final molar ratios of DCPD: W and DCPD: Al kept at 1200: 1 and 1200: 20, respectively; Then, the resulting dispersions were pushed by high-pressure nitrogen to the buffer bottle and mixed well by the mixing head. Finally, the mixed dispersions were pumped by vacuum pump to the mold, followed by curing for 1 h at 80°C.

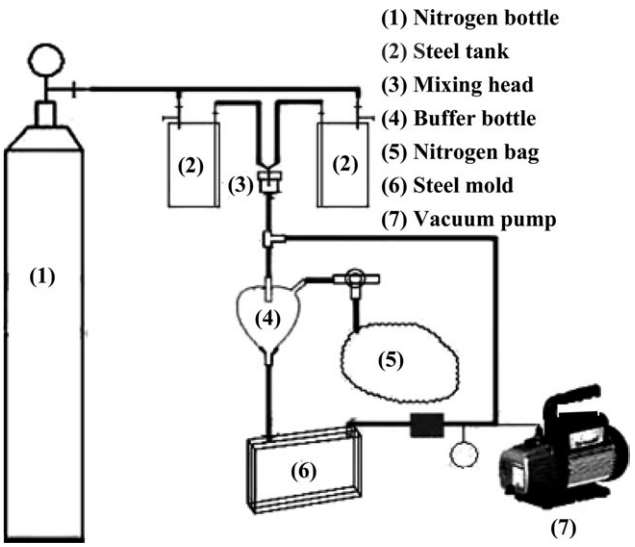

Figure 1. Simulating RIM device made in our lab.

Mechanical and Tribological Property Tests

The samples were prepared by universal system prototype (WZY-24) according to the Chinese standards. Tensile and bending properties were recorded on a universal testing machine (WDW-10) at room temperature. Impact strength was tested on an impact tester (XJU-22). The Shore D hardness was tested on a Shore durometer (XHS-D). Each value reported was the average of at least six samples.

The friction and wear behaviors of the nanocomposites sliding against steel were evaluated on a high-temperature and atmosphere QG-700 model ball-on-disk tester against GCr15 steel ball under dry sliding condition. The diameter of the steel spherical ball used was 5 mm, and its chemical composition was C: 0.95–1.05%, Si: 0.15–0.35%, Mn: 0.25–0.45%, Cr: 1.40–1.65%, S $\leq$ 0.025%, P $\leq$ 0.025%, Mo $\leq$ 0.10%, Ni $\leq$ 0.30%, Cu $\leq$ 0.25%, and Ni + Cu $\leq$ 0.05%. The tests were carried out at a velocity of 800 rev/min, sliding velocity of 0.419 m/s, load of 20 N, and duration of 60 min at room temperature. Before each test, the steel ball and the polymer disk were abraded with No. 600 water-abrasive paper to reach a surface roughness. Then, the material was cleaned with ethanol-dipped cotton. For every group, three samples were selected, and the friction coefficient was the average result of the three repetitions. Then, the specific wear rate of the specimen was calculated from the following relationship:

$$W = \iiint_v dxdydz/(L \times N) = \frac{2\pi}{3} Rbh/(L \times N)$$

where W is the specific wear rate (mm^3/Nm), R is the semidiameter of the steel ring (mm), b is the width of the wear trace (mm), h is the depth of the wear trace (mm), L is the sliding distance in meters, and N is the load in Newtons. The width and depth of the wear trace were obtained from the 3D surface topography images of worn surfaces by the *Nano*focus procedure.

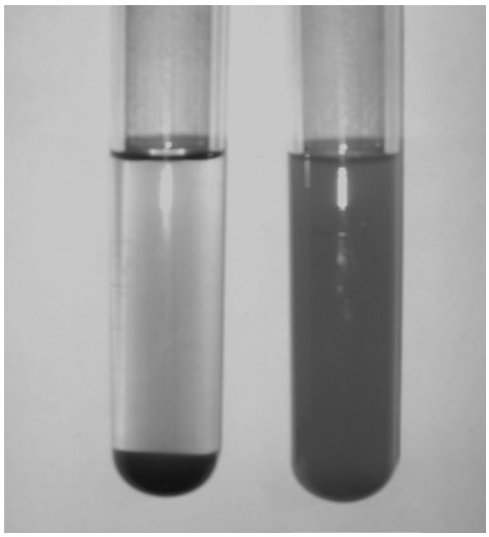

Figure 2. Setting test of pristine and PyDDP-hybridized MoS_2 in DCPD monomer (left, pristine MoS_2 in DCPD monomer after 30 min; right, PyDDP-hybridized MoS_2 in DCPD monomer after 2 days). [Color figure can be viewed in the online issue, which is available at wileyonlinelibrary.com.]

Analysis of the Specimens

Thermogravimetric analysis (TGA) was performed using a JEOL DSC6200 thermal analyzer at a heating rate of 10°C min^{-1} in nitrogen with a continuous purge of air. Fourier transform infrared spectroscopy (FTIR) spectra were obtained from a NEXUS Thermo Nicolet Fourier transform spectrum. Samples were prepared as pellets using spectroscopic grade KBr. Scanning electron microscopy (SEM) examinations on a JSM-6700F was used to study the morphology of impact fracture surfaces and furthermore the morphology of worn surfaces, counterpart surface, and worn debris. The width and depth of the wear trace were obtained from the 3D surface topography images of worn surfaces by the *Nano*focus procedure. The dispersion of MoS_2 in the PDCPD matrix was taken using a Hitachi S-4800 field emission scanning electron microscopy (FESEM).

RESULTS AND DISCUSSION

Structural Characterization of MoS_2 Fillers

It was not possible to create well-dispersed suspensions of pristine MoS_2 in DCPD monomer because of poor compatibility. As shown in Figure 2(a), when pristine MoS_2/DCPD suspensions were removed from the sonication bath, the pristine MoS_2 agglomerated and settled to the bottom immediately. To obtain uniform distribution in the monomer, PyDDP was grafted on the surface of MoS_2 particles using the procedures described above (see Experimental Section), with the expectation of improved interfacial compatibility between the MoS_2 and the DCPD monomer. As in Figure 2(b) indicated, the surface modified MoS_2 particles hybridized with PyDDP were easily dispersed in DCPD monomer once sonication started and remained stable indefinitely.

Figure 3(a) illustrates the FTIR absorption spectra of the PyDDP and PyDDP-hybridized MoS_2 particles. In the spectrum

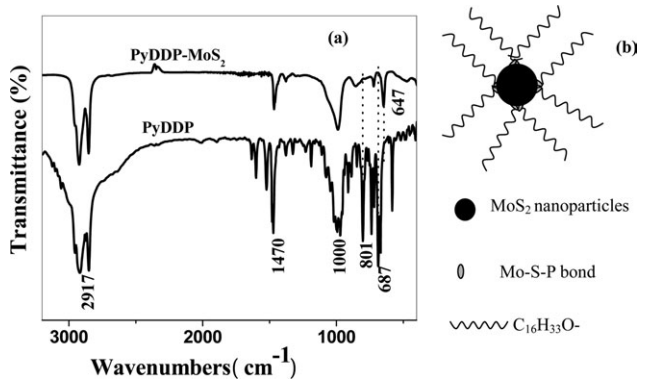

Figure 3. (a) FTIR spectra of PyDDP-hybridized MoS_2 (top) and PyDDP (bottom) and (b) the structural diagram of PyDDP-hybridized MoS_2 nanoparticles.

of PyDDP [Figure 3(a), bottom], the absorption bands at 2917 and 1470 cm^{-1} were typical of compounds with long-aliphatic chains; the peak around 1000 cm^{-1} was attributed to the stretching band of P—O bond; and the sharp peak at 801 cm^{-1} appeared was known to be the P=S stretching band. After the grafting reaction, the FTIR spectrum of PyDDP-hybridized MoS_2 particles apparently changed [Figure 3(a), top]; the most obvious changes were the disappearance of the P=S vibration band at 801 cm^{-1} and the peak shift from 687 to 647 cm^{-1}. The disappearance of the peak at 801 cm^{-1} implied the reaction occurred between the P=S bond of PyDDP molecule and the Mo atom on the surface of MoS_2 nanoclusters; the peak shift was related to the conjugate structure of P—S—Mo.[28] FTIR results indicated that PyDDP was covalently grafted on the surface of MoS_2 nanoparticles by the chemical bond of P—S—Mo. Accordingly, the structural diagram of PyDDP-hybridized MoS_2 nanoparticles is illustrated in Figure 3(b).

TGA was performed to verify the thermal stability and extent of grafting of PyDDP-hybridized MoS_2 nanoparticles (Figure 4).

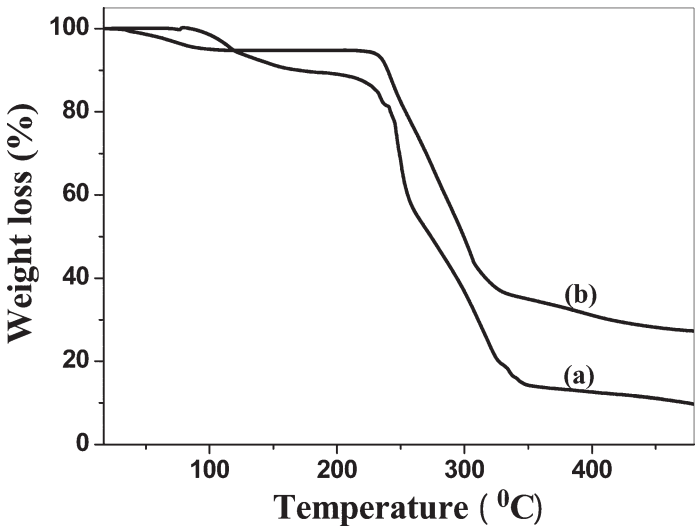

Figure 4. Thermogravimetric analysis (TGA) weight loss curves of (a) PyDDP and (b) PyDDP-hybridized MoS_2 nanoparticles.

Applied Polymer SCIENCE

As in Figure 4 indicated, the PyDDP-hybridized MoS_2 decomposed gradually with increasing temperature and showed a higher decomposition onset temperature compared to PyDDP, which implied that PyDDP was covalently connected on the surface of MoS_2 nanoparticles. For the PyDDP-hybridized MoS_2 nanoparticles, there existed significant weight loss between 230 and 330°C (onset was at 230°C) that could be attributed to the decomposition of the grafted PyDDP. Accordingly, the grafting degree of the PyDDP hybridized to the surface of MoS_2 nanoparticles was estimated from TGA as 57.2 wt % (at 330°C).

Impact Fractured Morphology of Nanocomposites

Figure 5 shows the SEM micrographs of the fracture surfaces of the pure PDCPD and MoS_2/PDCPD composites. Compared with the fracture surface of the pristine MoS_2/PDCPD composites [Figure 5(b)], the surfaces of the pure PDCPD [Figure 5(a)] and PyDDP-hybridized MoS_2/PDCPD nanocomposites [Figure 5(c)] showed much smoother, implying the PyDDP-hybridized MoS_2 nanoparticles were homogeneously dispersed into the PDCPD matrix. Conversely, the crack pinning or crack deviation was also found in the fracture surface of PyDDP-hybridized MoS_2/PDCPD nanocomposites [Figure 5(c)], which indicated a higher energy consumption of the nanocomposites during fracture and expected the superior mechanical properties of the nanocomposites. Furthermore, the much more rough fracture surface for pristine MoS_2/PDCPD composites [Figure 5(b)] indicated that cracks traveled at high speed, allowing less matrix deformation because time for yielding was limited. Impeded matrix deformation reduced flexural strength and failure strain and yielded an embrittling effect.[29]

Mechanical Performance of Nanocomposites

All mechanical properties tested of the MoS_2/PDCPD nanocomposites with various MoS_2 loadings are tabulated in Table I. It was clearly shown that the addition of PyDDP-hybridized MoS_2 enhanced the tensile strength and modulus of the nanocomposites. When the content of MoS_2 was increased to 1 wt %, the tensile strength and modulus of the nanocomposites attained the highest value. With further increase of MoS_2 loadings, the tensile strength and modulus of the nanocomposites decreased slightly, but still higher than those of the pure PDCPD. Similarly, the flexure and impact properties of the nanocomposites were also improved by the addition of modified MoS_2. The enhancement of mechanical properties of MoS_2/PDCPD nanocomposites were possibly due to that of the entangled chains formed between PyDDP and the PDCPD matrix, here MoS_2 acted as the crosslink point, resulting in the increase of crosslinking degree of the nanocomposites. However, the crosslinking degree of MoS_2/PDCPD nanocomposites would decrease when the content of MoS_2 was higher than 1 wt %, which was caused by the effect of polymerization retardation of MoS_2 nanoparticles Therefore, the mechanical performance decreased with the further increase of MoS_2 loadings. In addition, the mixing of MoS_2 also enhanced the hardness of the nanocomposites. It was attributed that the hardness of MoS_2 particles was higher than the pristine PDCPD matrix; conversely, the well-dispersed MoS_2 nanoparticles in the PDCPD matrix could act as the rigid support point and undertake loading effectively.

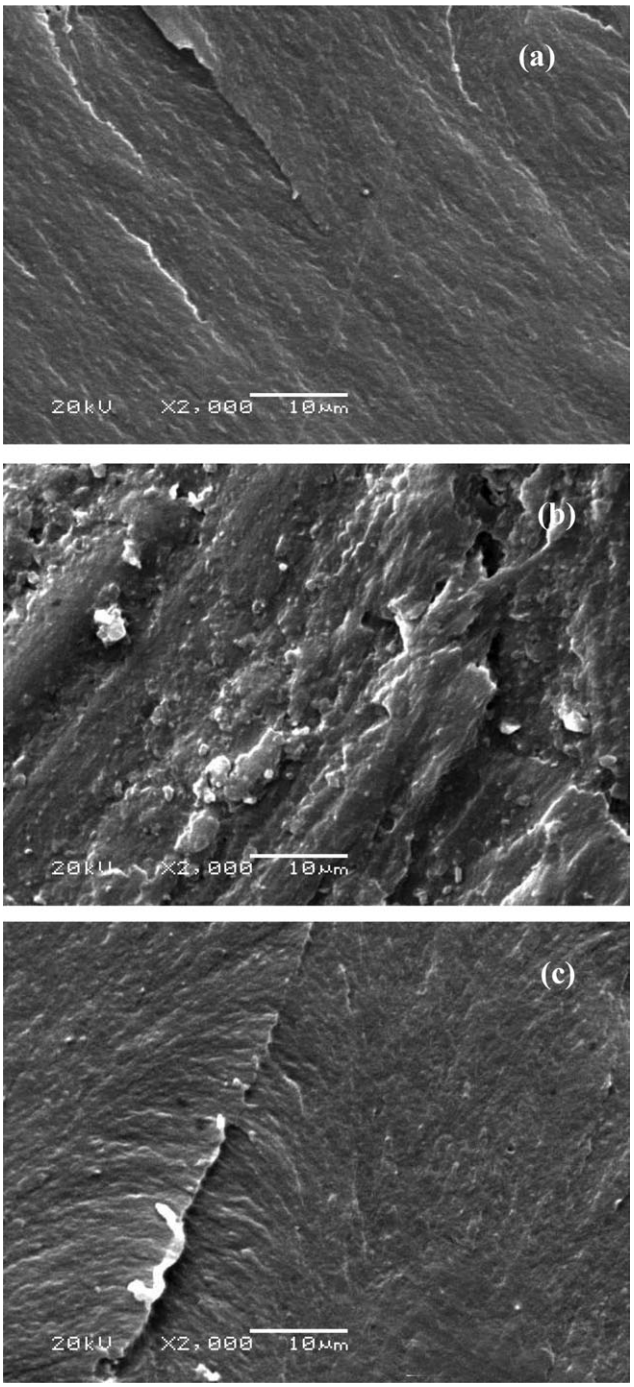

Figure 5. SEM micrographs of impact fractured surface for (a) pure PDCPD, (b) pristine MoS_2/ PDCPD, and (c) PyDDP-hybridized MoS_2/ PDCPD nanocomposites.

Compared to the pristine MoS_2/PDCPD composites with 1 wt % MoS_2 loading, the tensile strength, tensile modulus, bending strength, bending modulus, and impact strength of PyDDP-hybridized MoS_2/PDCPD nanocomposites with the same MoS_2 loading increased 49.9, 89.1, 24.4, 67.0, and 17.8%, respectively. It was obviously clear that the surface modification of MoS_2 particles played an important role in the mechanical behavior, which implied that the interfacial compatibility between the

Table I. The Effect of MoS_2 Loading on Mechanical Properties of the MoS_2/PDCPD Nanocomposites

MoS_2	Doped percentage (%)	Tensile strength (MPa)	Tensile modulus (MPa)	Bending strength (MPa)	Bending modulus (MPa)	Impact strength (J/m)	Shore D hardness (°)
PyDDP-hybridized	0	35.5	1171	58.6	1846	45	75.1
	0.5	46.8	1316	65.2	2310	50	78.8
	1	53.2	2214	72.9	3083	53	79.6
	2	41.8	1920	65.3	2517	48	79.1
Pristine	1	29.8	1259	50.6	2105	38	78.4

particle/matrix interfaces was very important for the polymer-based composites.

Tribological Property of Nanocomposites

Analysis of the Friction Coefficient and Specific Wear Rate. The friction coefficient of MoS_2/PDCPD nanocomposites filled with various amount of PyDDP-hybridized MoS_2 is shown in Figure 6. It was shown that the addition of MoS_2 obviously decreased the friction coefficient of MoS_2/PDCPD nanocomposites. With the further increase of MoS_2 loadings, the friction coefficient of nanocomposites increased slightly, but still lower than that of pristine PDCPD when the loadings of MoS_2 reached 2 wt %. The results of friction coefficient demonstrated that the addition of MoS_2 improved the wear resistance of PDCPD, and the MoS_2/PDCPD nanocomposites filled with 1 wt % MoS_2 exhibited the best anti-wear ability.

Analysis of specific wear rate is also one of the powerful methods in polymer tribology research. As in Figure 7 indicated, the specific wear rate decreased with the increase of MoS_2 loadings from 0.5 to 1 wt %; the further increase of MoS_2 content greater than 1 wt % resulted in the increasing of specific wear rate. These results also indicated that the MoS_2/PDCPD nanocomposites filled with 1 wt % MoS_2 exhibited the best anti-wear property, which was in accordance with that from the analyses of friction coefficient. It was clearly that the wear resistance of materials had a close relation with its mechanical performance and hardness (Table 1). Similar results were also reported by Zhao et al.,[30] in the study of modified carbon fibers reinforced polyurethane of best anti-wear ability. This is due to the mechanical properties of the composites improved by the addition of carbon fiber. Accordingly, the improvement in the wear resistance of MoS_2/PDCPD nanocomposites could be attributed to the improved mechanical performance and hardness by the addition of MoS_2 particles. The increasing of specific wear rate when the loadings of MoS_2 nanoparticles were greater than 1 wt % might result from the slight decrease in mechanical performance and hardness of MoS_2/PDCPD nanocomposites.

Morphology of Worn Surface and Counterpart Surface. The morphology of worn surfaces provides visible evidence for the improved wear resistance of the MoS_2/PDCPD nanocomposites. To understand the effect of MoS_2 on the friction and wear behaviors of the MoS_2/PDCPD nanocomposites, the morphologies of the worn surfaces as well as counterpart steel spherical ball were investigated. Figure 8 demonstrates the SEM images of the worn surfaces of the pristine PDCPD [Figure 8(a)], the MoS_2/PDCPD nanocomposites filled with 1 wt % MoS_2 [Figure 8(c)], and the corresponding steel counterpart surfaces [Figure 8(b) and (d)] under the same friction condition. The arrows indicated the sliding direction in the figure. For the worn surface of pure PDCPD [see Figure 8(a)], more scuffing and plastic deformation marks could be found on the worn surface; and little debris was adhered on the worn surface. While for the MoS_2/PDCPD nanocomposites with 1 wt % MoS_2 loading [see Figure 8(c)], its worn surface was relatively smooth and the plough marks were nearly invisible; merely a great amount of

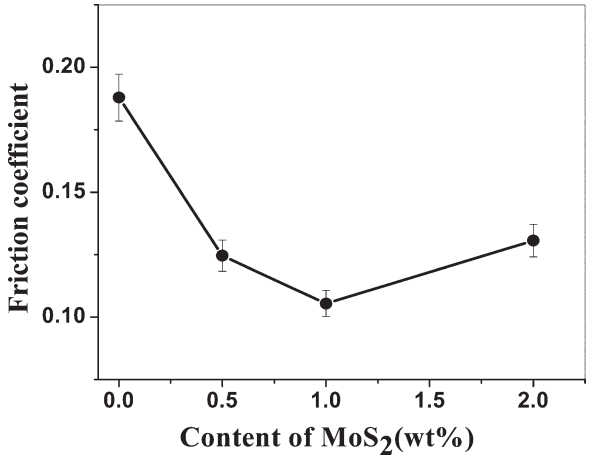

Figure 6. Variation of friction coefficient of MoS_2/PDCPD nanocomposites with the loading of MoS_2 under dry sliding.

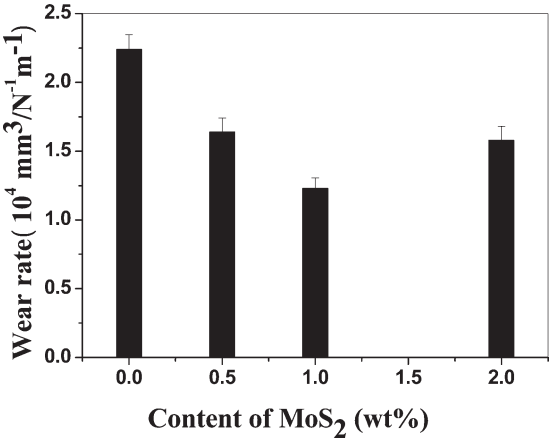

Figure 7. Variation of specific wear rate of MoS_2/PDCPD nanocomposites with the loading of MoS_2 under dry sliding.

Applied Polymer SCIENCE

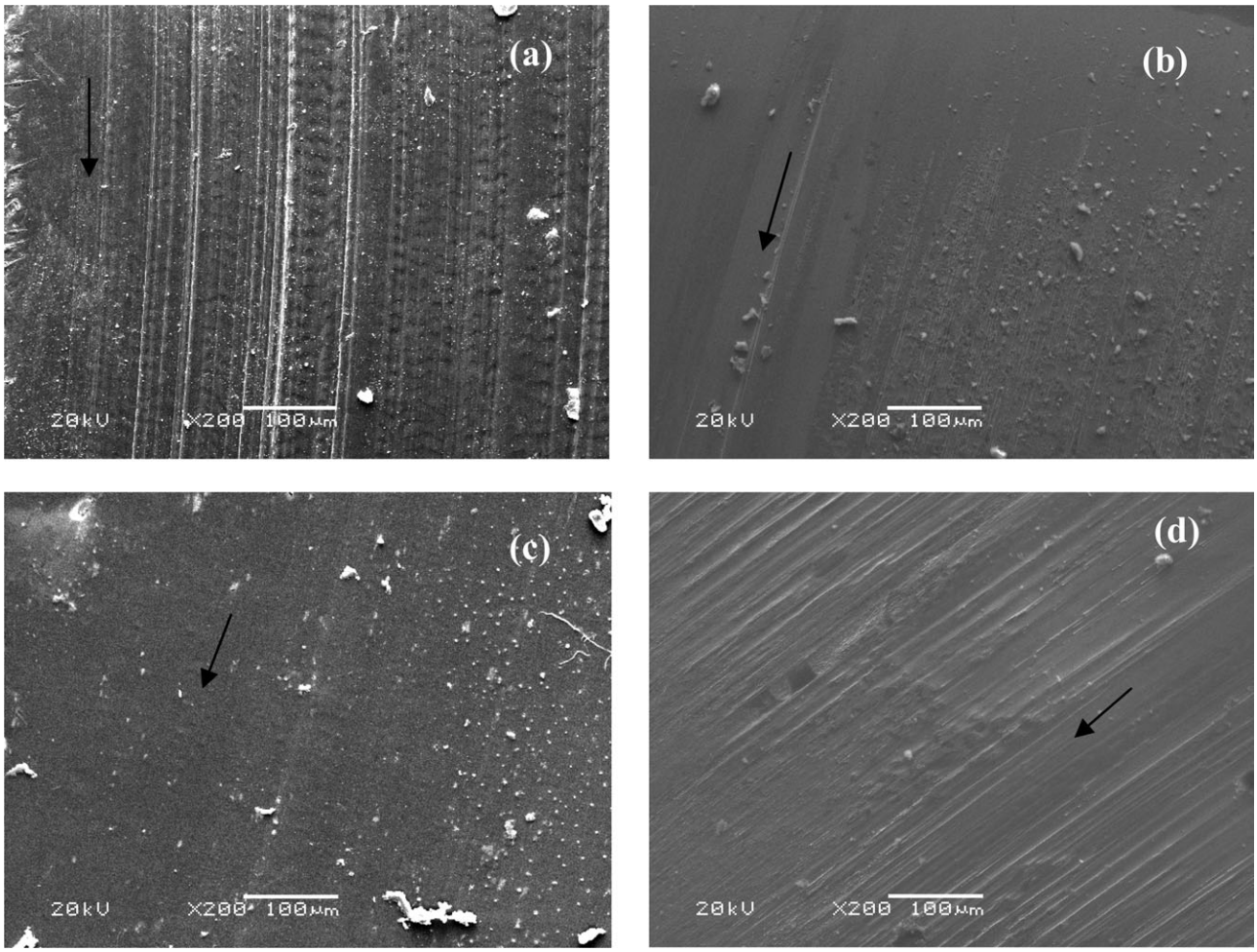

Figure 8. SEM images of the worn surfaces and counterpart surfaces of MoS_2/PDCPD nanocomposites with various amount of MoS_2 sliding against steel. (a) worn surface of pure PDCPD; (b) counterpart surface of pure PDCPD; (c) worn surface of 1 wt % MoS_2 loading; and (d) counterpart surface of 1 wt % MoS_2 loading.

debris was adhered on the worn surface acting as lubricants. The SEM images of worn surfaces obviously indicated that the MoS_2/PDCPD nanocomposites showed better wear resistance than the pure PDCPD. Conversely, analysis of counterpart steel spherical ball also provides important information on tribological property in polymer tribology research. Compared to the pristine PDCPD [see Figure 8(b)], serious scratches were found on the counterpart steel spherical ball surface of MoS_2/PDCPD nanocomposites [see Figure 8(d)]. This was caused by the friction cutting effect of MoS_2 nanoparticles on the counterpart steel spherical ball. Generally speaking, the more serious the counterpart steel spherical ball, the better the wear resistance of materials. The results were consistent with those obtained by the morphologies analysis of worn surfaces of nanocomposites, further proved the friction and wear properties of MoS_2/PDCPD nanocomposites were better than those of pure PDCPD.

Morphology of Wear Debris. Analysis of wear debris is one of the powerful methods in polymer tribology research.[31,32] Figure 9 shows the SEM pictures of the wear debris of pristine PDCPD and MoS_2/PDCPD nanocomposites filled with 1 wt % MoS_2. Generally, wear debris produced during sliding process can be attributed to an abrasive microcutting effect.[33] The asperities of the harder surface of the steel ring exert a ploughing action on the softer materials and then the debris is produced. It seemed from Figure 9(a) that the morphology of the debris appeared fiber-like aggregates, and the size of the aggregates was in the micrometer scale; whereas for the MoS_2/PDCPD nanocomposites filled with 1 wt % MoS_2, the debris presented flake-like particles morphology and the average particle size was dramatically decreased compared to that of pure PDCPD. These phenomena also indicated the better wear resistance of MoS_2/PDCPD nanocomposites than pristine PDCPD, which was in accordance with the previous conclusions.

Generally speaking, the anti-wear ability is not only related to the lubricating property, but also the mechanical properties of the materials. For the pure PDCPD, its lubricating property was poor due to the low hardness and carrying capacity. With the increasing of MoS_2 loadings, the distribution of MoS_2 nanoparticles in the PDCPD matrix became continues grid. Thus, one layer lubricating film on the surface of PDCPD could be formed, which effectively decreased the friction coefficient of

MoS_2/PDCPD nanocomposites due to the superior lubricating property of MoS_2 itself. Conversely, the addition of MoS_2 enhanced the hardness of the nanocomposites; accordingly, the carrying capacity of the MoS_2/PDCPD nanocomposites was improved, which was also in favor of decreasing the friction coefficient of MoS_2/PDCPD nanocomposites. Therefore, the wear resistance of MoS_2/PDCPD nanocomposites was better than that of pristine PDCPD.

Dispersion of MoS_2 Nanoparticles in PDCPD Matrix

To further confirm the good dispersion of MoS_2 nanoparticles in the PDCPD matrix, field emission scanning electron measurements are required. The FESEM images of the pure PDCPD and MoS_2/PDCPD nanocomposites fractures obtained under liquid nitrogen are shown in Figure 10. Compared with the pristine PDCPD [Figure 10(a)], Figure 10(b) presented clearly a continuous matrix with uniform distributing MoS_2 nanometer phase, indicating the good dispersion of MoS_2 nanoparticles in PDCPD matrix. As indicated from the arrows, the average size of MoS_2 in the matrix was about 100–150 nm, which was larger than that of PyDDP-hybridized MoS_2 nanoparticles observed under TEM. It was due to the size of PyDDP was also included

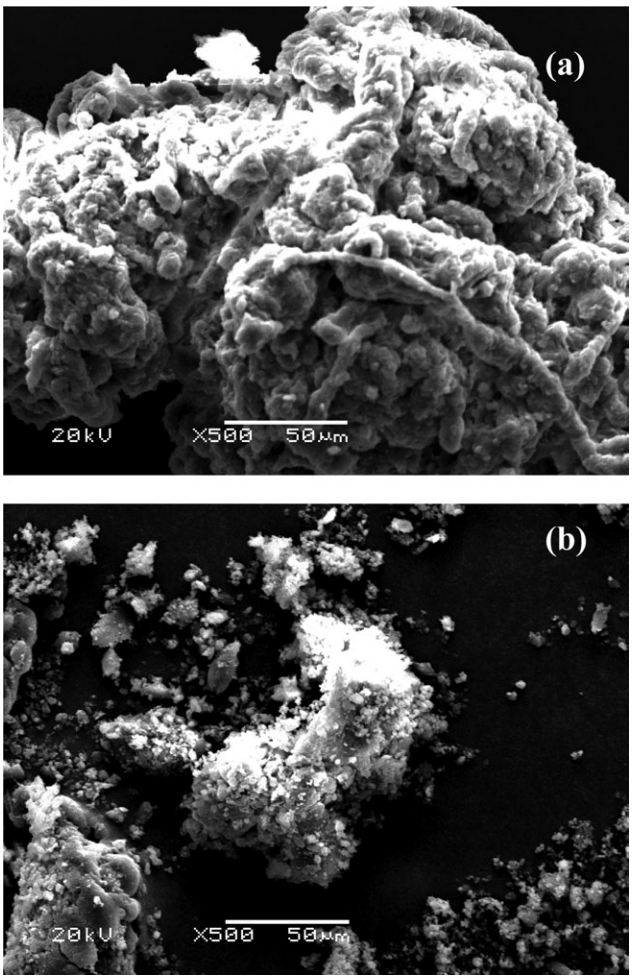

Figure 9. SEM micrographs of the wear debris of (a) pure PDCPD and (b) MoS_2/PDCPD nanocomposites filled with 1 wt % of MoS_2 under dry sliding.

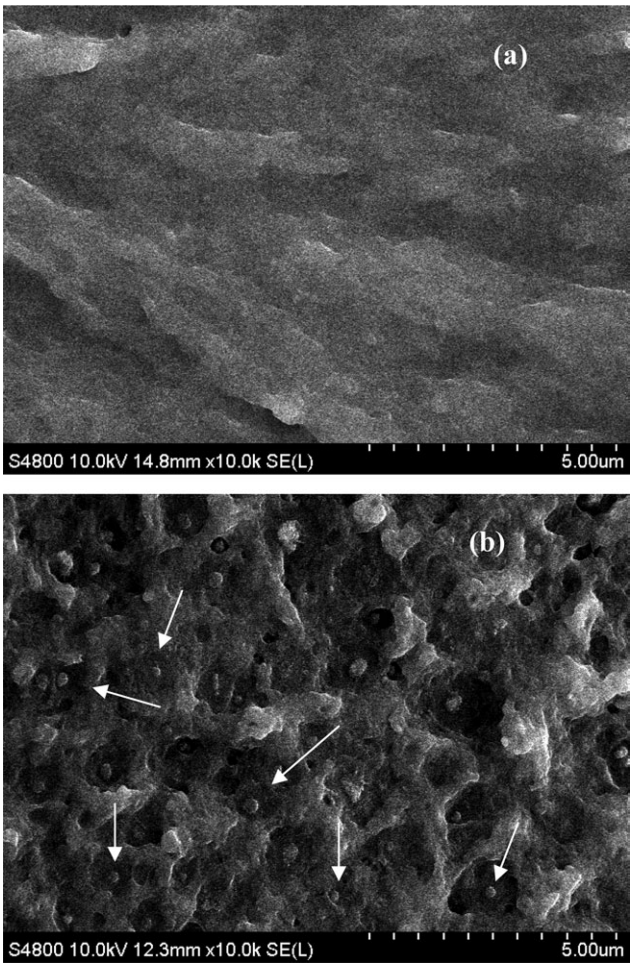

Figure 10. FESEM images of (a) pure PDCPD and (b) MoS2/PDCPD nanocomposites with 1 wt % of MoS2 loading.

by SEM observation. Based on the FESEM observations, it could be concluded that the addition of MoS_2 into the PDCPD matrix created a nanoscale heterogeneous structure; majority of the MoS_2 nanoparticles was uniformly dispersed in PDCPD matrix. These results suggested that there existed favorable interfacial compatibility between PyDDP-hybridized MoS_2 nanoparticles and PDCPD matrix, which was in accordance with the previous conclusion obtained from the dispersion experiment of MoS_2 nanoparticles in DCPD.

It is well known that the well-interfacial compatibility plays an important role to effectively improve the mechanical and tribological properties of polymer-based materials.[34,35] The improved mechanical and tribological properties of MoS_2/PDCPD nanocomposites could be attributed to the good dispersion of PyDDP-hybridized MoS_2 nanoparticles in the PDCPD matrix, which effectively decreased interfacial energy and reinforced interfacial interaction between MoS_2 nanoparticles and PDCPD matrix. But when the loadings of MoS_2 were above 1%, the inevitable deterioration in mechanical and tribological properties of nanocomposites was arising from the decreased crosslinking degree in the PDCPD matrix, which was caused by the polymerization retardation of MoS_2 nanoparticles.

CONCLUSIONS

The MoS_2/PDCPD nanocomposites with the improved mechanical and wear resistance properties were successfully prepared by means of *in situ* ROMP using RIM process. It was possible to achieve a homogeneous dispersion by grafting PyDDP onto the MoS_2 surface by *in situ* surface grafting method. The addition of MoS_2 improved the mechanical performance; meanwhile, obviously decreased the friction coefficient and enhanced the wear resistance of the PDCPD. The MoS_2/PDCPD nanocomposites with 1 wt % MoS_2 loading exhibited the best mechanical and anti-wear performance. FESEM results indicated the PyDDP-hybridized MoS_2 nanoparticles uniformly dispersed in PDCPD matrix. The well-interfacial compatibility between the particle/matrix interfaces played an important role for the improved mechanical and tribological properties of the MoS_2/PDCPD nanocomposities in very low MoS_2 loadings.

ACKNOWLEDGMENTS

This work was financially supported by National Natural Science Foundation of China (No. 21101058).

REFERENCES

1. Gaurav, A.; Ashamol, A.; Deepthi, M. V.; Sailaja, R. R. N. *J. Appl. Polym. Sci.* **2012**, *125*, E16.
2. Abdullateef, A. A.; Thomas, S. P.; Al-Harthi, M. A.; Bandyopadhyay, Sri; De, S. K.; Basfar, A. A.; Atieh, M. A. *J. Appl. Polym. Sci.* **2012**, *125*, E76.
3. Luo, F.; Chen, L.; Ning, N.; Wang, K.; Chen, F.; Fu, Q. *J. Appl. Polym. Sci.* **2012**, *125*, E348.
4. Perez, L. D.; Lopez, B. L. *J. Appl. Polym. Sci.* **2012**, *125*, E327.
5. Zhuang, G. S.; Sui, G. X.; Meng, H.; Sun, Z. S.; Yang, R. *Comp. Sci. Technol.* **2007**, *67*, 1172.
6. Veena, M. G.; Renukappa, N. M.; Suresha, B.; Shivakumar, K. N. *Polym. Compos.* **2011**, *32*, 2038.
7. Hu, Y.; Zhou, S.; Wu, L. *Polymer* **2009**, *50*, 3609.
8. Lin, O. H.; Akil, H. M.; Mohd Ishak, Z. *Polym. Compos.* **2011**, *32*, 1568.
9. Brostow, W.; Deborde, J. -L.; Jaklewicz, M.; Olszynski, P. *J. Mater. Ed.* **2003**, *25*, 119.
10. Myshkin, N. K.; Petrokovets, M. I.; Kovalev, A.V. *Tribol. Int.* **2005**, *38*, 910.
11. Brostow, W.; Kovacevic, V.; Vrsaljko, D.; Whitworth, J. *J. Mater. Ed.* **2010**, *32*, 273.
12. Brostow, W.; Datashvili, T.; Kao, D.; Too, J. *Polym. Compos.* **2010**, *31*, 417.
13. Gilman, J. W.; Jackson, C. L.; Morgan, A. B.; Harris, R. H. *Chem. Mater.* **2000**, *12*, 1866.
14. Jeong, W.; Kessler, M. R. *Chem. Mater.* **2008**, *20*, 7060.
15. Hamming, L. M.; Qiao, R.; Messersmith, P. B.; Catherine Brinson, L. *Comp. Sci. Technol.* **2009**, *69*, 1880.
16. Chen, J. H.; Rong, M. Z.; Ruan, W. H.; Zhang, M. Q. *Comp. Sci. Technol.* **2009**, *69*, 252.
17. He, J.; Li, H.; Wang, X.; Gao, Y. *Eur. Polym. J.* **2006**, *42*, 1128.
18. Wang, Z.; Li, H.; He, B. *Polym. Mater. Sci. Eng.* **2000**, *16*, 93 (in Chinese).
19. Woodson, C. S.; Grubbs, R. H. U.S. Pat. 6020443 (**2000**).
20. Mitra, Y.; Hossein, T.; William, L. K. *Macromolecules* **2004**, *37*, 2511.
21. Amendt, M. A.; Chen, L.; Hillmyer, M. A. *Macromolecules* **2010**, *43*, 3924.
22. Yu, W.; Wang, J.; Dong, H. China Pat. 201010004829.0 (**2010**).
23. Lu, C.; Liu, J.; Liu, X. *AcMCS* **2011**, *28*, 35.
24. Pan, B.; Xing, Y.; Zhang, C.; Zhang, Y. *Adv. Mater. Res.* **2010**, 123–125, 231.
25. Yang, G.; Ma, H. Z. *Mater. Rev.* **2003**, *17*, 63.
26. Hu, K. H.; Liu, M.; Wang, Q. J.; Xu, Y. F.; Schraube, S.; Hua, X. G. *Tribol. Int.* **2009**, *42*, 33.
27. Zhang, Z. J.; Zhang, J.; Xue, Q. J. *J. Phys. Chem.* **1994**, *98*, 12973.
28. Chen, S.; Liu, W.; Yu, L. *Wear* **1998**, *218*, 153.
29. Wetzel, B.; Haupert, F.; Zhang, M. Q. *Comp. Sci. Technol.* **2003**, *63*, 2055.
30. Zhao, G.; Wang, T.; Wang, Q. *Polym. Compos.* **2011**, *32*, 1726.
31. Chen, Z.; Li, T.; Yang, L.; Liu, X.; Lv, R. *Wear* **2004**, *257*, 696.
32. Song, H. J.; Zhang, Z. Z. *Mat Sci Eng A* **2006**, *242*, 340.
33. Wang, H. -G.; Mu, B.; Ren, J. -F.; Jian, L. -Q.; Zhang, J. -Y.; Yang, S. -R. *Polym. Compos.* **2009**, *30*, 1326.
34. Kopczynska, A.; Ehrenstein, G. W. *J. Mater. Ed.* **2007**, *29*, 325.
35. Desai, R. C.; Kapral, R. Dynamics of Self-organized and Self-assembled structures; Cambridge University Press: Cambridge, New York, **2009**.